



ELSEVIER

Available online at [www.sciencedirect.com](http://www.sciencedirect.com)

SCIENCE @ DIRECT®

Journal of Magnetism and Magnetic Materials 294 (2005) e73–e76



[www.elsevier.com/locate/jmmm](http://www.elsevier.com/locate/jmmm)

# Magnetic properties of TiO<sub>2</sub> rutile implanted with Ni and Co

J.V. Pinto<sup>a,b,c</sup>, M.M. Cruz<sup>a,\*</sup>, R.C. da Silva<sup>b,d</sup>, E. Alves<sup>b,d</sup>, M. Godinho<sup>a</sup>

<sup>a</sup>*Departamento de Física/CFMC-UL, FCUL, Campo Grande, Ed. C8, 1749-016 Lisboa, Portugal*

<sup>b</sup>*LFI, Departamento de Física, ITN, E.N. 10, 2686-953 Sacavém, Portugal*

<sup>c</sup>*Departamento de Física/FCT-UNL, FCUL, Monte da Caparica, 2829-516 Caparica, Portugal*

<sup>d</sup>*CFNUL, Av. Prof. Gama Pinto 2, 1649-003 Lisboa, Portugal*

Available online 18 April 2005

## Abstract

Single crystals of TiO<sub>2</sub> rutile were implanted with high fluences of Co and Ni ions, aiming at the understanding of the role of these ions in the magnetic properties of the doped oxide. Magnetization and electrical resistivity results as a function of temperature and magnetic field are presented and correlated with information obtained by Rutherford backscattering spectrometry measurements in the same samples.

© 2005 Elsevier B.V. All rights reserved.

*PACS:* 75.50Cc; 75.50Tt

*Keywords:* Implanted insulators; Rutile; TiO<sub>2</sub>; Magnetic nanoparticles

TiO<sub>2</sub> is a very stable oxide used in a large range of technological applications. The possibility of being a suitable material for spintronics was opened when Co doped TiO<sub>2</sub> anatase thin films were reported to be ferromagnetic semiconductors at room temperature [1]. Since then, TiO<sub>2</sub> doped with cobalt has been extensively studied, mainly in thin film configuration, both in anatase and rutile forms. In this work, we study cobalt doped and

nickel doped rutile in order to understand the influence of the magnetic dopant.

Co and Ni ions were introduced into {100} rutile single crystals using ion implantation technique with an energy of 150 keV and fluences of  $2 \times 10^{17} \text{ cm}^{-2}$ . The as-implanted samples were analyzed by Rutherford backscattering spectrometry (RBS) to access the depth distribution of the implanted ions. To characterize the magnetic behavior of the samples, magnetization measurements were carried out as a function of temperature, between 4 and 400 K, under magnetic fields up to 5.5 T, using a SQUID magnetometer. Electrical resistivity was also measured between

\*Corresponding author. Tel.: +351 21 7500912;  
fax: +351 21 7500977.

*E-mail address:* [mmcruz@fc.ul.pt](mailto:mmcruz@fc.ul.pt) (M.M. Cruz).

10 and 300 K using a standard 4-point probe technique.

The RBS results show that the maximum local concentrations of dopant ions and the thicknesses of the implanted regions are 27 at% and 130 nm for Ni, and 23 at% and 105 nm for Co, respectively.

Zero field cooled (ZFC) and field cooled (FC) magnetization curves for the as-implanted samples were measured in a field of 5 mT. Since the implanted layer corresponds to a very small fraction of the samples volume ( $<0.02\%$ ), the contribution of the unimplanted rutile was subtracted in order to isolate the behavior of the implanted region. To do so, unimplanted crystals were also characterized. The experimental results show that the magnetic behavior of those unimplanted crystals can be described by a Van Vleck paramagnetic component (the value of the measured susceptibility agrees with published results [2]), added with a small ferromagnetic component attributed to impurities.

The results for the magnetic moment of the as-implanted samples, already corrected for the contribution of the unimplanted volume, are presented in Fig. 1. These results are similar to those obtained for nickel and cobalt implanted MgO, with local atomic concentrations of the order of 15 at% [3], and suggest the existence of metallic aggregates. The formation of cobalt aggregates was also reported in reduced cobalt doped rutile films [4].

In nickel-implanted samples, the behavior can be indexed as superparamagnetic, indicating that the size of the aggregates is in the range of a few nanometers. This is confirmed by the presence of a maximum in the ZFC magnetic moment, indicating a blocking at a temperature  $T_B = 50$  K, and by the fact that, above this maximum, the dependence can be described by a Curie–Weiss law, with ionic magnetic moments of the order of  $100 \mu_B$ , a value too high for individual ions.

Accordingly, the magnetic moment scales with  $H/T$  above  $T_B$ , the dependence being well fitted with a Langevin function (Fig. 2). The saturated magnetic moment is found to be  $0.2 \mu_B/\text{Ni}$  ion, indicating that 33% of the implanted ions are in aggregates, assuming the same saturation

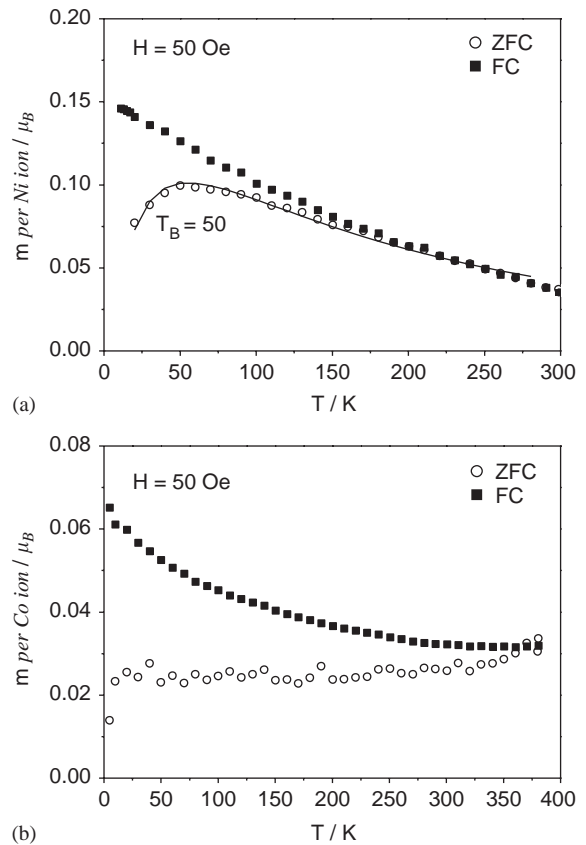


Fig. 1. ZFC and FC magnetic moment versus temperature for the as-implanted samples: (a) Ni, (b) Co. The results were subtracted for the unimplanted region contribution. The solid line in (a) is the result of the theoretical fit.

magnetization as in the bulk metal. From both the temperature and field dependence results, assuming a log-normal distribution of magnetic moments, an average diameter of 8 nm (corresponding to an average magnetic moment of  $17000 \mu_B$ ) and an anisotropy constant of  $1.8 \times 10^4 \text{ J m}^{-3}$  are deduced. The standard deviation obtained for the log-normal distribution is  $\sigma = 1.1$ . The anisotropy constant value is higher than the corresponding metal bulk value  $K_{\text{eff}}(\text{FCC Ni}) = -K_1/12 = 1 \times 10^4 \text{ J m}^{-3}$ . This is expected since the anisotropy constants generally increase for smaller nanoparticles, due to surface contribution.

For the cobalt implanted  $\text{TiO}_2$  rutile, assuming a similar behavior, the evolution of the

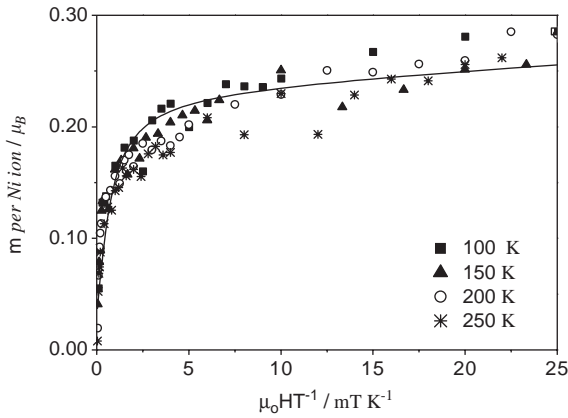


Fig. 2. Magnetic moment per nickel ion versus applied field divided by temperature for temperatures between 100 and 300 K for the sample implanted with 150 keV Ni. The results were subtracted for the unimplanted region. The solid line is the fitted Langevin behavior assuming a log-normal distribution of magnetic moments.

magnetization indicates a blocking temperature at or above 380 K. The fact that ZFC and FC results join at 380 K indicates that the  $T_B$  value should not be far. Below this temperature, the  $M(H)$  curves exhibit a saturated magnetic moment of  $0.75 \mu_B/\text{Co}$  ion, constant up to 300 K, while the coercive field decreases markedly with temperature. This behavior is characteristic of the existence of nanosized aggregates. The same analysis as in nickel allows concluding that a fraction of about 43% of the implanted cobalt is in aggregate form. Since the anisotropy constant cannot be accessed due to the high value of the blocking temperature, the Co bulk anisotropy constants are used to estimate an upper limit for the particle average volume,  $V$ . Using  $K_{\text{eff}}V = 30k_B T_B$  and  $K_{\text{eff}} = -K_1/12 = 2 \times 10^4 \text{ J m}^{-3}$ , in the case of FCC cobalt, or  $K_{\text{eff}} = -K_1 = 2.5 \times 10^5 \text{ J m}^{-3}$  in the case of HCP cobalt, the limiting values for the particle diameters are 25 (FCC Co) and 11 nm (HCP Co), respectively.

The electrical resistance,  $R$ , was measured as a function of temperature to characterize the electrical behavior of the implanted regions. The electrical resistivity,  $\rho$ , was determined using  $\rho = R \times \pi t / \ln 2$ , where  $t$  is the thickness of the implanted region (Fig. 3). Although the RBS

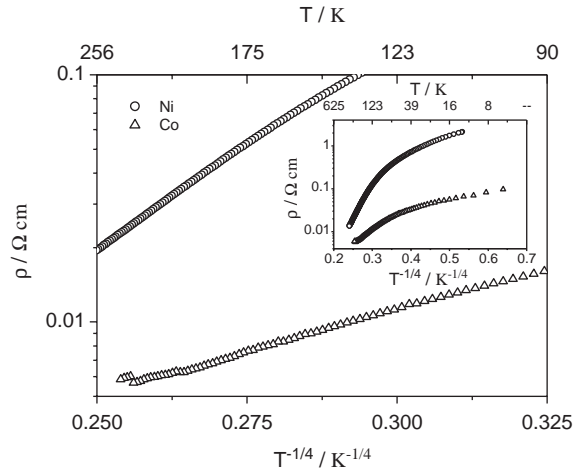


Fig. 3. Electrical resistivity as a function of  $T^{-1/4}$  for the as-implanted samples evidencing the variable range hopping behavior above 100 K. The inset presents the variation in the whole range of temperatures.

results indicate that the implanted region is highly amorphized the obtained electrical resistivity cannot be explained as due to implantation defects alone. The values obtained at room temperature for the electrical resistivity of cobalt and nickel doped samples are  $5 \times 10^{-3}$  and  $2 \times 10^{-2} \Omega \text{ cm}$ , respectively. These values are lower than the ones obtained for rutile implanted with noble gases at high fluences, 1.6 and  $3.3 \Omega \text{ cm}$  for Xe and Ar, respectively (notice that the electric conductivity of  $\text{TiO}_2$  saturates with ion fluence in these cases) [5]. The resistivity values in our systems are attributed then to the combination of implantation induced defects and the presence of the magnetic ions.

As seen from the inset in Fig. 3, the whole temperature dependence cannot be described by a single mechanism. Above 100 K, the logarithm of  $\rho$  is linear in  $T^{-1/4}$ , indicating that transport occurs by variable range hopping. This model describes a thermally activated transport through localized electronic states with a disordered distribution. In our samples, the localization of electronic states is a consequence of the large amorphization induced during implantation. For temperatures lower than 100 K, the ionization of impurities is a dominant mechanism.

To study the possible magnetoresistive effects, electrical resistivity was also measured under applied magnetic field up to 5.5 T. No significant differences could be detected between the measurements performed with and without applied magnetic field, in the whole range of temperatures.

In conclusion, we showed that after ion implantation nanometer sized magnetic Co and Ni particles are formed in rutile. In the case of cobalt, the ordered magnetic behavior is exhibited up to temperatures above room temperature. In both cases, the implanted ions do not induce any magnetoresistive effects in rutile. The detailed characterization of the so-formed aggregates and the study of their stability and evolution under thermal treatments are in progress.

### Acknowledgments

This work is partially supported by the Portuguese foundation FCT, through a Ph.D. grant (BD/8907/2002) to J.V. Pinto.

### References

- [1] Y. Matsumoto, M. Murakami, T. Shono, T. Hasegawa, T. Fukumura, M. Kawasaki, P. Ahmet, T. Chikyow, S. Koshihara, H. Koinuma, *Science* 291 (2001) 854.
- [2] F.E. Senftle, T. Pankey, F.A. Grant, *Phys. Rev.* 120 (1960) 820.
- [3] J.V. Pinto, M.M. Cruz, R.C. da Silva, E. Alves, R. González, M. Godinho, *Eur. Phys. J. B*, to appear.
- [4] S.R. Shinde, S.B. Ogale, J.S. Higgins, H. Zheng, A.J. Millis, V.N. Kulkarni, R. Ramesh, R.L. Greene, T. Venkatesan, *Phys. Rev. Lett.* 92 (2004) 166601.
- [5] R. Fromknecht, I. Khubeis, S. Massing, O. Meyer, *Nucl. Instrum. Methods B* 147 (1999) 191.